Electronic Supplementary Material (ESI) for Nanoscale.

Supporting Information

Two-Dimensional Conductive Polymer/V_2O_5 Composite with Rapid Zinc-Ion Storage Kinetics for High-Power Aqueous Zinc-Ion Battery

Bo Wang,‡[a] Simin Dai,‡[c] Zehao Zhu,‡[c] Lin Hu,[b] Zhen Su,[b] Yingzhi Jin,[b] Liukang Xiong,[c] Jiasong Gao,[c] Jun Wan,*[c,d] Zaifang Li,*[b] and Liang Huang*[c]

[a] School of Electrical Engineering and Automation, Luoyang Institute of Science and Technology, Luoyang 471023, China.

[b] China-Austrialia Institute for Advanced Materials and Manufacturing, Jiaxing University, Jiaxing 314001, China.

[c] Wuhan National Laboratory for Optoelectronics, Huazhong University of Science and Technology, Wuhan 430074, China.

[d] State Key Laboratory of New Textile Materials and Advanced Processing Technologies, Hubei Key Laboratory of Biomass Fibers and Eco-Dyeing & Finishing, Wuhan Textile University, Wuhan 430200, China.

‡ These authors contributed equally to the work.

* Corresponding authors. E-mail addresses: wanj@wtu.edu.cn (J. Wan); zaifang.li@zjxu.edu.cn (Z. Li); huangliang421@hust.edu.cn (L. Huang)

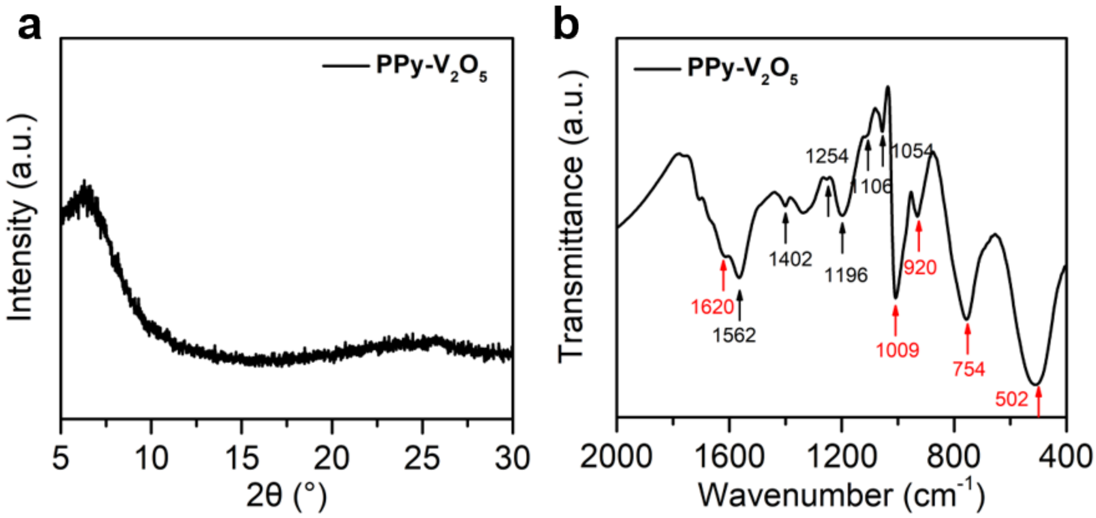

Fig. S1. (a) XRD pattern and (b) FTIR spectra of PPy/V_2O_5.

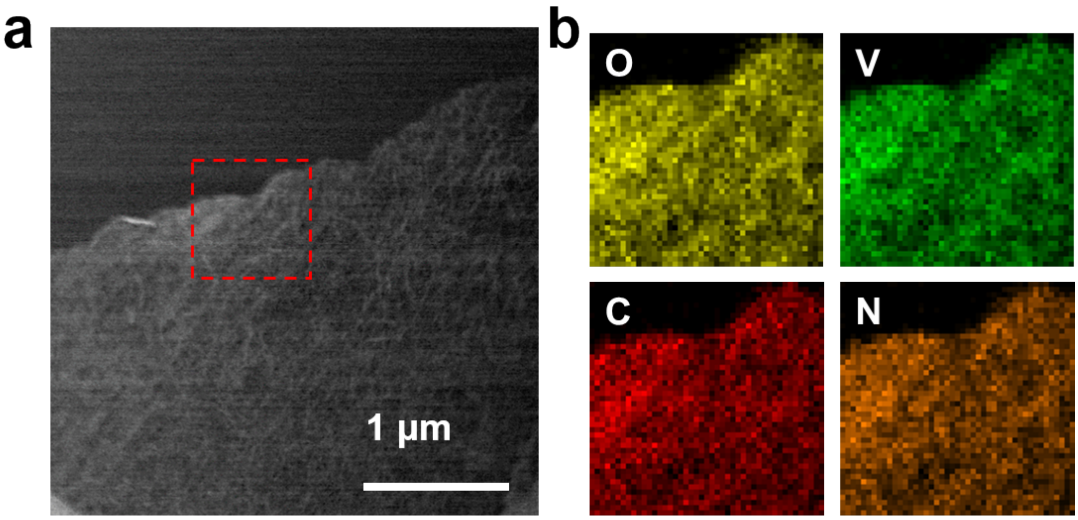

Fig. S2. (a) TEM image and (b) the corresponding elements mapping of PPy/V_2O_5, showing the distribution of O, V, C, and N in the material.

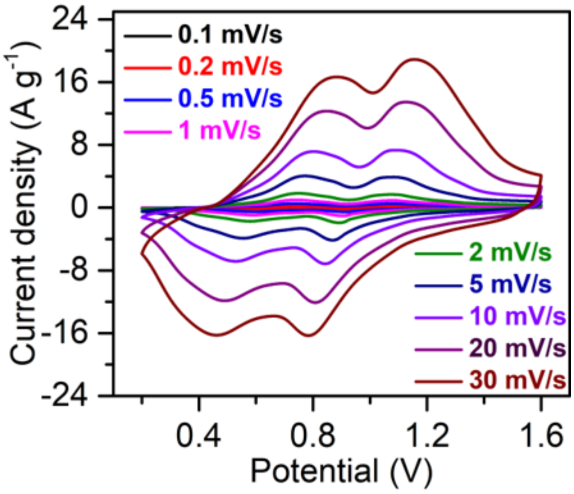

Fig. S3. CV curves at different scan rates.

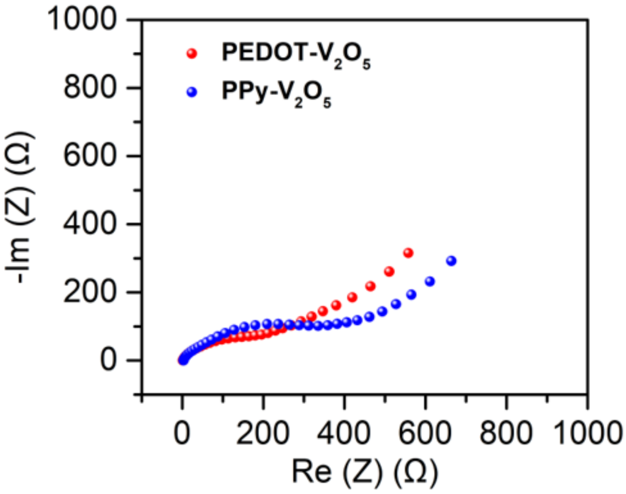

Fig. S4. The electrochemical impedance spectroscopy curves of PEDOT/V_2O_5 and PPy/V_2O_5.

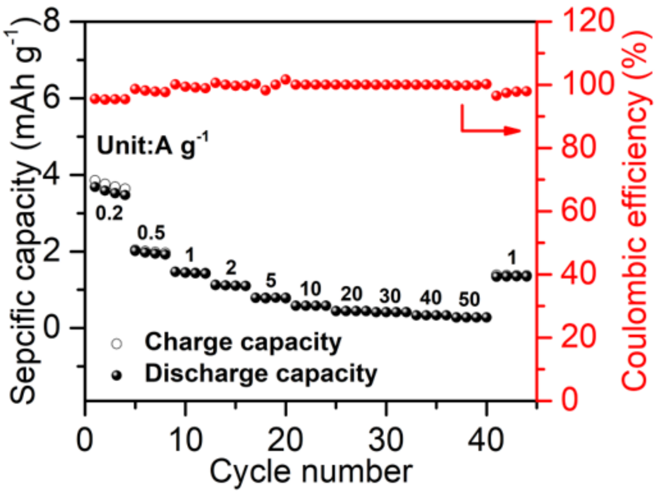

Fig. S5. Rate capabilities of PEDOT at different rates from 0.2 to 50 A g^{-1}.

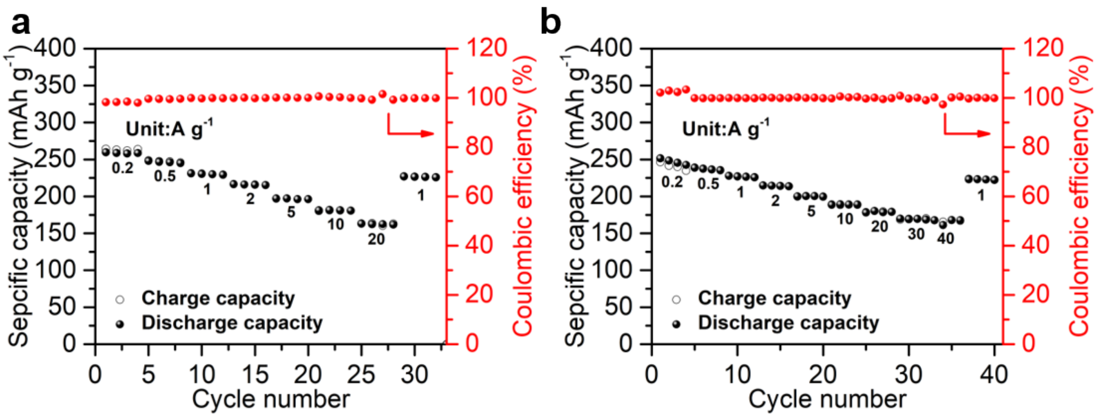

Fig. S6. Rate capabilities of (a) PEDOT/V_2O_5-1 and (b) PEDOT/V_2O_5-2 at different rates from 0.2 to 50 A g^{-1}.

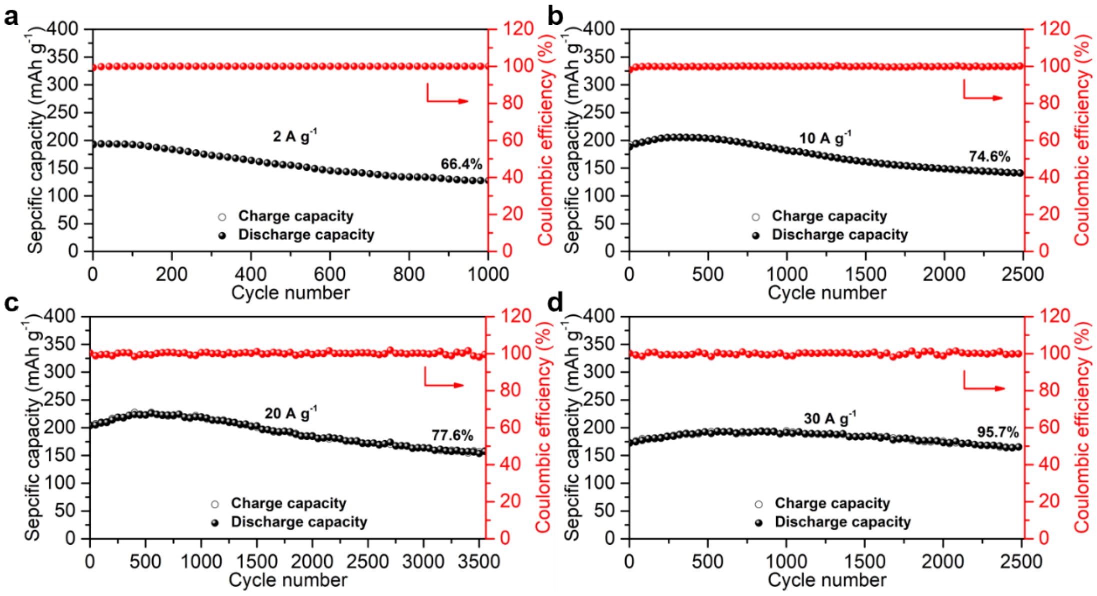

Fig. S7. Cyclic performances of PEDOT/V_2O_5 at (a) 2 A g^{-1}, (b) 10 A g^{-1}, (c) 20 A g^{-1}, and (d) 30 A g^{-1}.

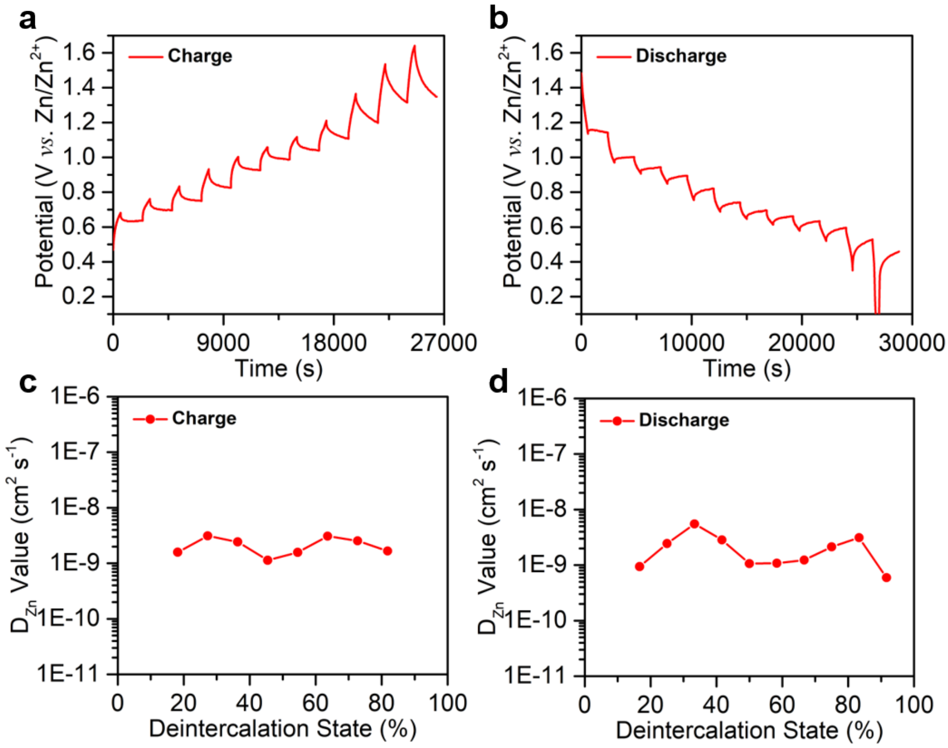

Fig. S8. (a, b) GITT analysis results for PPy/V_2O_5 in charge/discharge process. (c, d) The Zn^{2+} diffusion coefficient at different states of charge/discharge obtained by GITT.

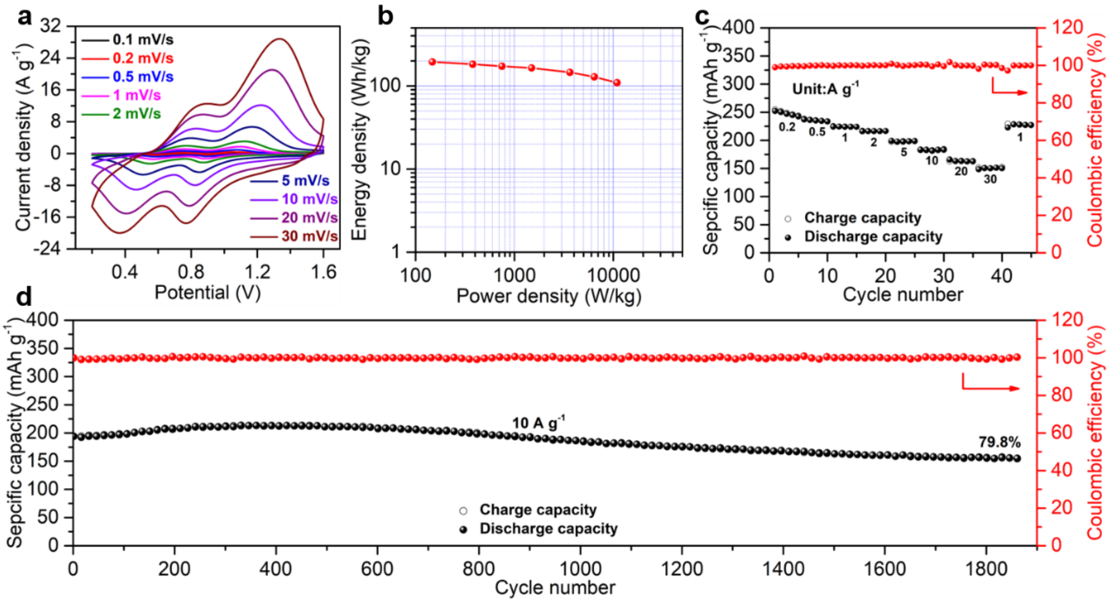

Fig. S9. (a) CV curves at different scan rates of PPy/V_2O_5 sample. (b) Ragone plots of aqueous Zn//PPy/V_2O_5 battery. (c) Rate capabilities of PPy/V_2O_5 at different rates from 0.2 to 30 A g^{-1}. (d) Cyclic performances of PPy/V_2O_5 at 10 A g^{-1} for 1800 cycles.

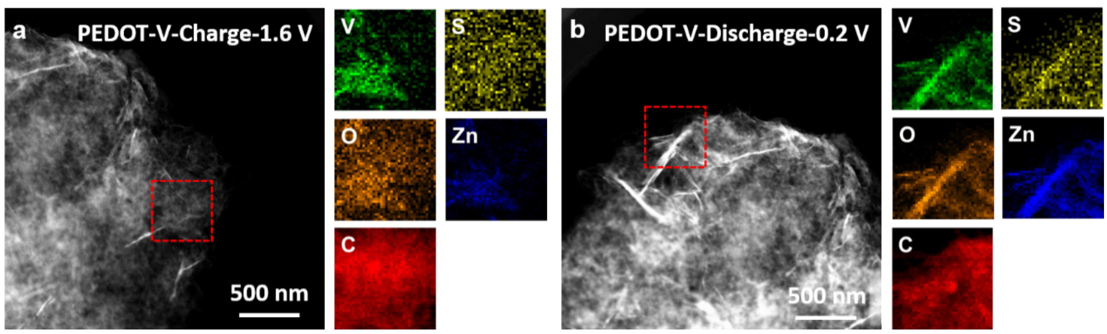

Fig. S10. The elements mapping of PEDOT/V_2O_5 at (a) fully charged state (1.6 V) and (b) fully discharged state (0.2 V).

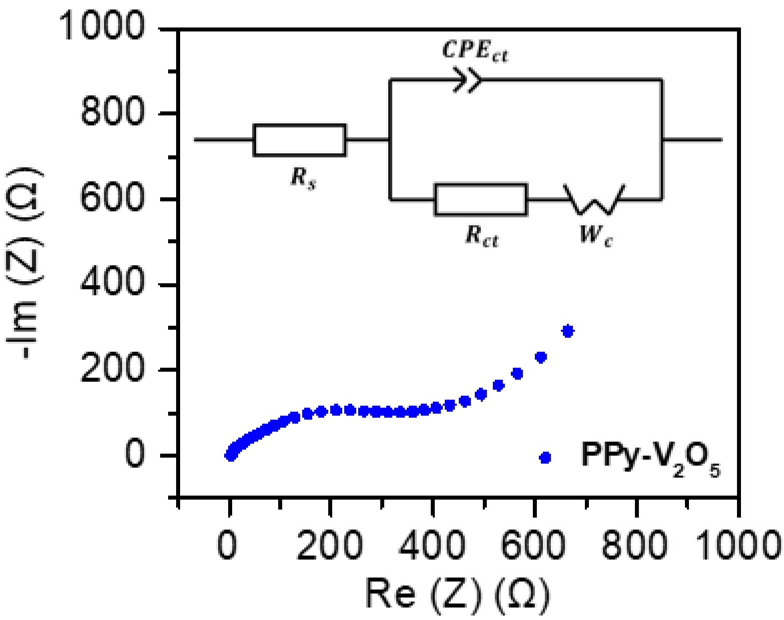

Figure 11. The equivalent circuit model of EIS of PPy/V_2O_5

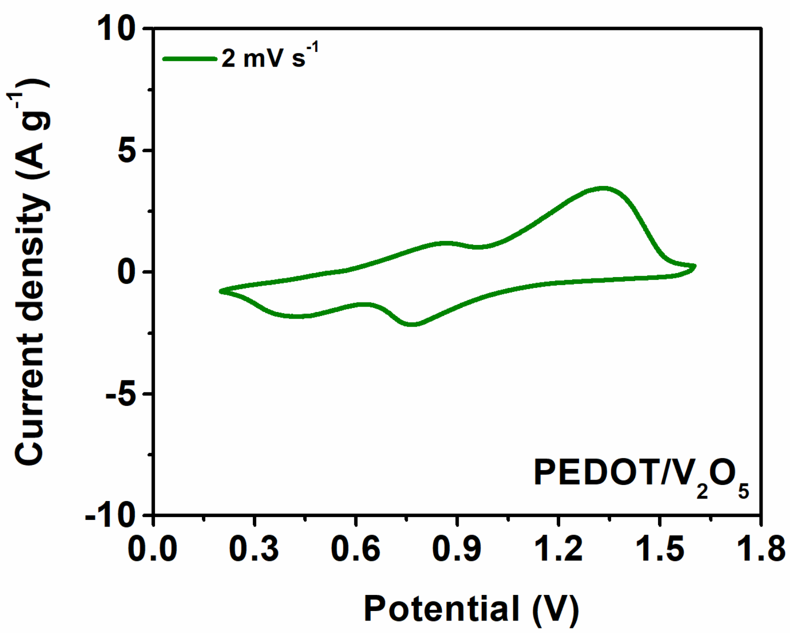

Figure 12. The CV curve of PEDOT/V_2O_5 at a scan rate of 2 mV s^{-1}

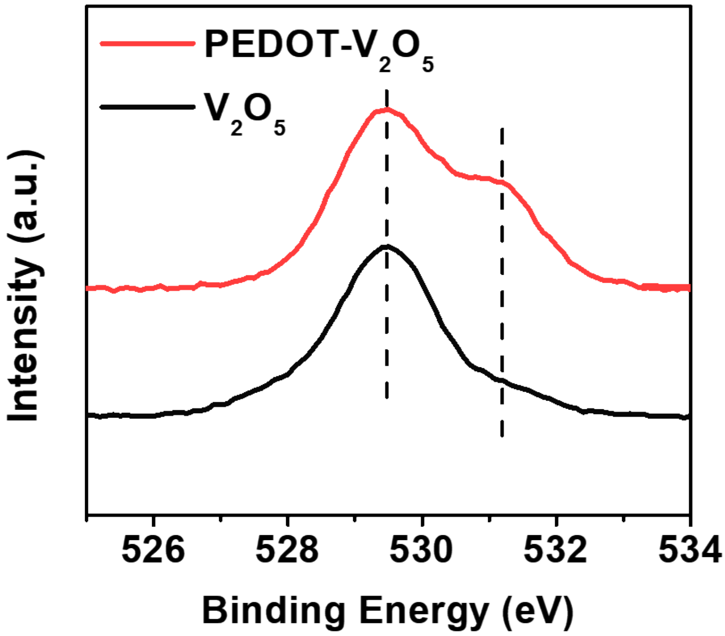

Figure S13. The high-resolution XPS O 1s spectra of pristine V_2O_5 and PEDOT/V_2O_5.

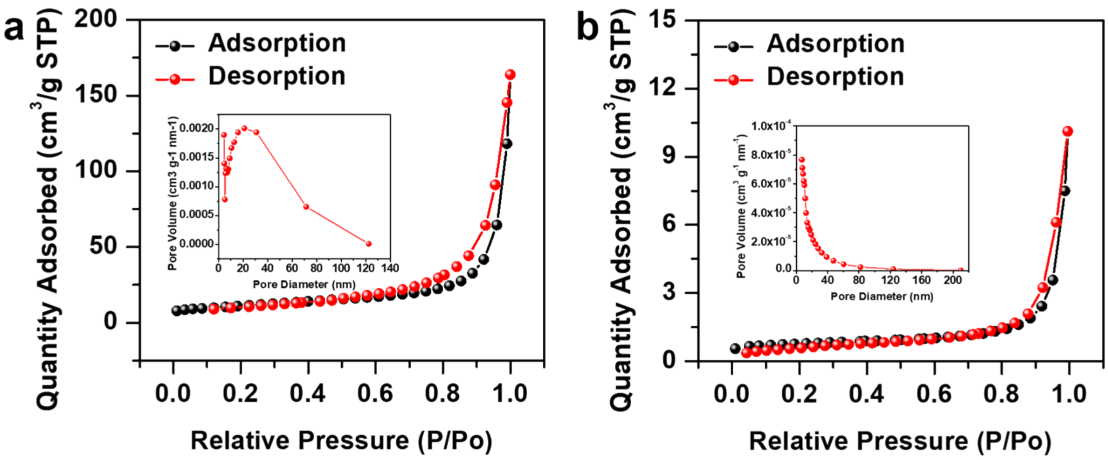

Figure S14. The N_2 adsorption–desorption isotherm and pore size distribution of (a) PEDOT-V_2O_5 and (b) pristine V_2O_5.